

Maintaining extraembryonic expression allows generation of mice with severe tissue factor pathway inhibitor deficiency

Michelle M. Castillo,^{1,2,*} Qihui Yang,^{1,*} Min Zhan,^{1,*} Amy Y. Pan,³ Michael W. Lawlor,¹ Alan E. Mast,^{2,4} and Rashmi Sood^{1,2}

¹Division of Pediatric Pathology, Department of Pathology, ²Department of Cell Biology, Neurobiology and Anatomy, and ³Quantitative Health Sciences, Department of Pediatrics, Medical College of Wisconsin, Milwaukee, WI; and ⁴Blood Research Institute, Blood Center of Wisconsin, Milwaukee, WI

Key Points

- Severe deficiency of TFPI K1 domain is compatible with embryonic development, adult survival, and reproductive functions in mice.
- Severely TFPI K1-deficient mice display elevated TAT levels, renal fibrosis, and increased susceptibility to TF-mediated pulmonary embolism.

Tissue factor pathway inhibitor (TFPI) is a serine protease with multiple anticoagulant activities. The Kunitz1 (K1) domain of TFPI binds the active site of factor VIIa and is required for inhibition of tissue factor (TF)/factor VIIa catalytic activity. Mice lacking TFPI K1 domain die in utero. TFPI is highly expressed on trophoblast cells of the placenta. We used genetic strategies to selectively ablate exon 4 encoding TFPI K1 domain in the embryo, while maintaining expression in trophoblast cells. This approach resulted in expected Mendelian frequency of TFPI K1 domain-deficient mice. Real-time polymerase chain reaction confirmed 95% to 99% genetic deletion and a similar reduction in transcript expression. Western blotting confirmed the presence of a truncated protein instead of full-length TFPI. Mice with severe TFPI K1 deficiency exhibited elevated thrombin-antithrombin (TAT) levels, frequent fibrin deposition in renal medulla, and increased susceptibility to TF-induced pulmonary embolism. They were fertile, and most lived normal life spans without any overt thrombotic events. Of 43 mice observed, 2 displayed extensive brain ischemia and infarction. We conclude that in contrast to complete absence of TFPI K1 domain, severe deficiency is compatible with in utero development, adult survival, and reproductive functions in mice. Inhibition of TFPI activity is being evaluated as a means of boosting thrombin generation in hemophilia patients. Our results show that in mice severe reduction of TFPI K1 activity is associated with a prothrombotic state without overt developmental outcomes. We note fibrin deposits in the kidney and rare cases of brain ischemia.

Introduction

Tissue factor pathway inhibitor (TFPI) is a serine protease inhibitor that regulates multiple steps in thrombin generation.¹ It is an efficient inhibitor of tissue factor (TF)/factor VIIa (fVIIa) catalytic activity. TFPI is highly expressed on trophoblast and endothelial cells of the placenta and in embryonic and adult tissues.²⁻⁵ It is alternatively spliced and produced in 2 major isoforms in humans, TFPI α and TFPI β . The longer isoform, TFPI α , consists of an acidic N-terminal region followed by 3 Kunitz-type domains, and a basic C-terminal region. The first and second Kunitz domains, respectively, bind the active sites of fVIIa and fXa,⁶ and the third Kunitz-type domain binds protein S.^{7,8} The C-terminal region of TFPI α contains a stretch of amino acids that bind fVa and promote inhibition of early forms of the prothrombinase complex.^{1,9,10} TFPI β lacks the third Kunitz domain and has an alternatively spliced C-terminal region that encodes a glycosylphosphatidyl inositol anchor, allowing surface association. The 2 isoforms differ in their distribution. In mice, both TFPI α and TFPI β are expressed in the placenta. TFPI α is also expressed by megakaryocytes, stored in platelets, and released upon platelet activation. Both α and β isoforms are expressed in mouse embryos, whereas adult mouse tissues predominantly express the TFPI β isoform.⁵

Submitted 20 March 2018; accepted 28 December 2018. DOI 10.1182/bloodadvances.2018018853.

*M.M.C., Q.Y., and M.Z. contributed equally to this work.

The full-text version of this article contains a data supplement.
© 2019 by The American Society of Hematology

Mice also produce a third TFPI isoform called TFPI γ . TFPI γ is a soluble form of TFPI containing only the first and second Kunitz domains and is widely expressed in mouse tissues. However, the production of TFPI γ protein has not been well characterized.¹¹

There are no documented cases of complete TFPI deficiency in humans. Reduced plasma levels are reported in FV-deficient patients^{12,13} and in patients lacking low-density lipoprotein, a carrier of TFPI in plasma.¹⁴ In mice, global deletion of exon 4 that encodes the K1 domain was reported to result in embryonic lethality. About 60% embryos were reported to die between 9.5 and 11.5 days of development with signs of yolk sac hemorrhage. The remaining embryos showed hemorrhage, particularly in the head, spine, and tail, accompanied by pallor. No live pups were found at birth.¹⁵ Thus, the most dramatic drop in the viability of TFPI K1 null embryos was observed soon after the formation of the definitive placenta. An independent study reported disruption of vascular network, thrombosis, and hemorrhage in placentas of late gestational TFPI_K1^{-/-} embryos.¹⁶ Based on these reports, we postulated a critical role of extraembryonic TFPI in inhibiting TF activity. The objectives of this study were to determine if maintaining extraembryonic expression allows in utero development of TFPI K1 domain-null embryos and to examine the effect of TFPI K1 deficiency on embryos and adult mice.

Methods

Mice

Animal experiments were conducted following standards and procedures approved by the Animal Care and Use Committee of the Medical College of Wisconsin. TFPI exon 4 floxed mice (stock number 017603; Jackson Laboratory, Bar Harbor, ME) and Meox2Cre mice (Stock number 003755; Jackson Laboratory) have been previously described.¹⁷⁻¹⁹ All mouse strains were used and maintained in C57BL/6 genetic background. Genetic combinations were generated by breeding and identified by polymerase chain reaction (PCR)-based genotyping of tissue obtained by tail biopsy. Primers described in original referenced publications or by Jackson Laboratory were used.

Analysis of pregnancies

The stage of pregnancies was assessed from days post coitum (dpc), assuming midday of plug as 0.5 dpc. Methods used for embryo dissection, genotyping, and phenotyping have been previously described.²⁰

Histology and immunohistochemistry

Organs were fixed in zinc formalin, embedded in paraffin, and cut into 4- μ m sections. Prior to embedding, the placentas were marked with ink to identify the center. Slides were stained with hematoxylin & eosin, Masson's trichrome, or Carstairs' stain (Electron Microscopy Sciences, Hatfield, PA) using standard protocols. For immunostaining, antigen retrieval was performed in citrate buffer pH 6.0, and antibodies that recognize macrophage marker F4/80 or neutrophil marker Ly-6G (ThermoFisher Scientific, Waltham, MA) were used.

Real-time PCR for genomic DNA and comparative expression analysis

Genomic DNA or total RNA was extracted from embryos or organs of adult mice. Total RNA was extracted using TRIZOL reagent

(ThermoFisher Scientific) and reverse transcribed with iScript cDNA Synthesis kit (Bio-Rad, Hercules, CA). Real-time quantitative PCR (qPCR) was performed with IQ SYBR Supermix (Bio-Rad) or a probe-based assay with primers designed to identify the presence of intact exon 4-5 (forward 5'-TCTGTTGCTTAGCCTTGTCC-3' and reverse 5'-CCATCATCTGCCTCATTGC-3') (expected product size 123 bp) or exon 7-8 (forward 5'-ACGTAGTCACTCATCTGTACCT-3' and reverse 5'-CAACCGCAACAACCTTTGAAAC-3') (expected product size 102 bp), using actin as internal control gene for normalization (forward 5'-AGGTCCTTACGGATGTCAACG-3' and reverse 5'-ATTGGCAACGAGCGGT-3') (Integrated DNA Technologies, Inc, Skokie, IL). Real-time qPCR with genomic DNA was performed with IQ SYBR Supermix (Bio-Rad) using TFPI forward 5'-AAGGGAACGAGAACCGATTT-3' and reverse 5'-AGAAACAA-CAGTGGGCCAGA-3' primers that amplify the intact gene but not exon 4-deleted gene. Internal positive controls for normalization were generated with forward 5'-CTAGGCCACAGAATTGAAAGATCT-3' and reverse 5'-GTAGGTGAAATTCTAGCATCATCC-3' primers. Following real-time analysis, the end products were separated on 1.8% agarose gels containing ethidium bromide and visualized by UV transillumination.

Western blot analysis

Mice were perfused with phosphate-buffered saline prior to organ harvest. Mouse tissues were weighed, minced, lysed, and centrifuged as previously described to remove cellular debris.⁵ For plasma sample preparation, 9 parts of blood was collected from the inferior vena cava into 1 part of 3.8% sodium citrate and 183 μ g/mL corn trypsin inhibitor. Plasma was separated by centrifugation at 200g for 5 minutes and then again at 800g for 10 minutes at room temperature. TFPI was precipitated from tissue lysates and plasma samples using bovine fXa coupled resin (ThermoFisher Scientific) and analyzed by sodium dodecyl sulfate-polyacrylamide gel electrophoresis and western blot using a rabbit anti-mouse TFPI polyclonal antibody. To allow a quantitative comparison, the weight or volume of TFPI K1-deficient and wild-type (WT) tissue or plasma samples, the volume of fXa coupled resin, and the volumes loaded on gels for each sample were kept equal.

Thrombin-antithrombin (TAT) levels and activity assays

Plasma TAT levels were measured using AssayMax Mouse TAT Elisa Kit (Assaypro LLC, St. Charles, MO) according to the manufacturer's instructions. Plasma was prepared by collecting 600 μ L blood from the inferior vena cava into 50 μ L of 16.5 mg/mL EDTA, followed by centrifugation at 1500g for 15 minutes. For thrombin generation assays, blood was drawn in sodium citrate, and platelet-poor plasma was diluted threefold before using it with Technothrombin TGA (Diapharma, West Chester, OH) as per the manufacturer's instructions. TF (RecombiPlasTin 2G; Instrumentation Laboratory, Bedford, MA) was reconstituted following the manufacturer's directions and used at a final dilution of 1:6000 for technothrombin assays.

TF-induced pulmonary embolism

TF (Recombiplastin 2G; Instrumentation Laboratory) was reconstituted according to the manufacturer's directions. Mice were weighed and anesthetized, and the inferior vena cava was exposed. A 1:80 dilution of TF (diluted in phosphate-buffered saline) was IV

Table 1. Pregnancy outcome of TFPI_K1^{Lox/Lox} female mice mated to Meox2Cre^{tg/+}TFPI_K1^{δ/+} male mice

Stage	TFPI_K1 ^{Lox/+}	TFPI_K1 ^{Lox/δ}	TFPI_K1 ^{δ/+}	TFPI_K1 ^{δ/δ}	No. aborted	No. analyzed (pregnancies)
12.5 dpc	6	11	13	6	4	40 (5)
15.5 dpc	4	4	9	5	3	22 (4)
Wean (~4 wk)	51	46	57	43*	—	197 (33)

Pregnancy outcome was analyzed at 12.5 dpc, at 15.5 dpc, and at wean ~4 wk of age. TFPI_K1^{δ/δ} mice survive embryonic development and are born at near expected frequency. No significant difference was observed from expected proportions at the time of wean, based on χ^2 GOF test ($P = .514$). Number aborted could not be determined when analysis was done at the time of weaning and is indicated by a dash.

*TFPI_K1^{δ/δ} pups were born at 22% frequency (95% CI 16% to 28%).

injected using a 26-gauge needle at a dose of 5 μ L/g body weight. Time to death was measured as time to the onset of respiratory arrest that lasted at least 2 minutes. All experiments were terminated at 30 minutes. The dose of TF used was selected by titration to be the lowest dose at which 80% of WT mice survived

beyond the 30-minute observation period. A previously described Evan's blue (1% in saline) perfusion assay and scoring system was used as an independent measure of lung vascular occlusion.²¹ One hundred percent of perfused lungs turned blue (score 0; no perfusion defect), whereas in the complete absence of perfusion,

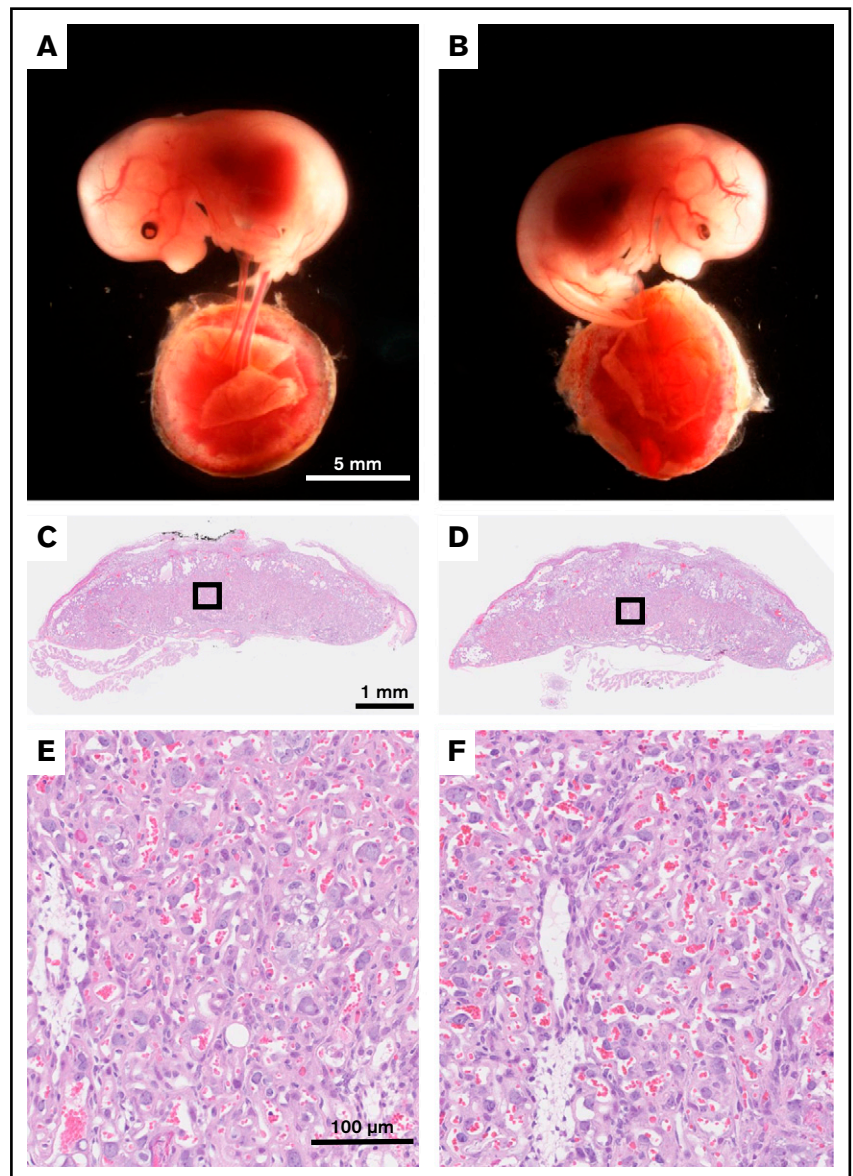


Figure 1. TFPI K1 domain-deficient embryos and placentas from epiblast-specific deletion appear grossly normal with no overt signs of hemorrhage. Representative images of littermate TFPI_K1^{δ/+} (A) and TFPI_K1^{δ/δ} (B) 15.5 dpc embryos and corresponding placentas among progeny of Meox2Cre^{tg/+} TFPI_K1^{δ/+} male mice mated to TFPI_K1^{Lox/Lox} female mice are shown. (C-D) Hematoxylin and eosin-stained sections of placentas shown in panels A and B, respectively. (E-F) Enlarged images of boxed regions in panels C and D, respectively. Maintaining expression of full-length TFPI in trophoblast cells corrects the abnormal vascularization observed in K1 null placentas.

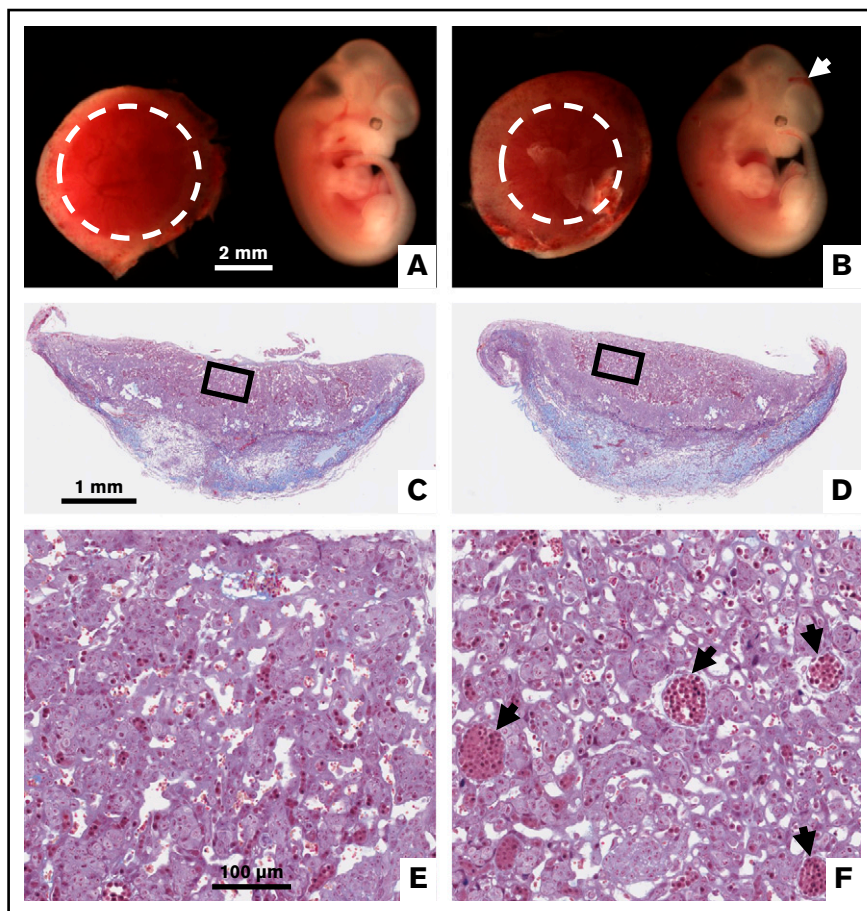


Figure 2. Intracranial hemorrhage and reduced placental vascularization in global TFPI K1 null embryos generated by TFPI_K1^{+/-} intercrosses. To replicate previously published observations with global deletion of TFPI K1 domain, we examined pregnancies from TFPI_K1^{+/-} intercrosses. Whole-mount images of 11.5 dpc TFPI_K1^{+/-} (A) and TFPI_K1^{-/-} (B) embryos and placentas are shown. The arrow points to intracranial hemorrhage of the TFPI_K1^{-/-} embryo. Labyrinth regions of placentas are highlighted with dotted circles; the placenta of the TFPI_K1^{-/-} embryo shows reduced labyrinth region. Carstairs' stained histological sections of both placentas are shown in panels C and D, and boxed regions are enlarged in panels E and F, respectively. Arrows point to large fetal vessels that may not have been optimally branched.

the lungs remained pink (score 4). Intermediate levels of perfusion were ranked as 1, 2, and 3 in the order of decreasing perfusion.

Statistical analysis

The χ^2 goodness-of-fit (GOF) test was used to determine deviation from expected Mendelian proportions. Exact binomial 95% confidence intervals (CIs) were computed where appropriate. The Student *t* test (2 tailed with unequal variance) was used for comparing TAT values and Evan's blue perfusion assay scores. Kaplan-Meier survival and Log-rank test were performed using SAS version 9.4 (SAS Institute, Cary, NC) and SPSS version 20.0 (IBM Corp, Armonk, NY). Two-proportion *z* test was used to compute *P* values for surviving proportions in TF-induced pulmonary embolism assay. *P* < .05 was used to establish significance for all experiments.

Results

TFPI Kunitz1 (K1) deficiency is compatible with embryonic development if placental expression is maintained

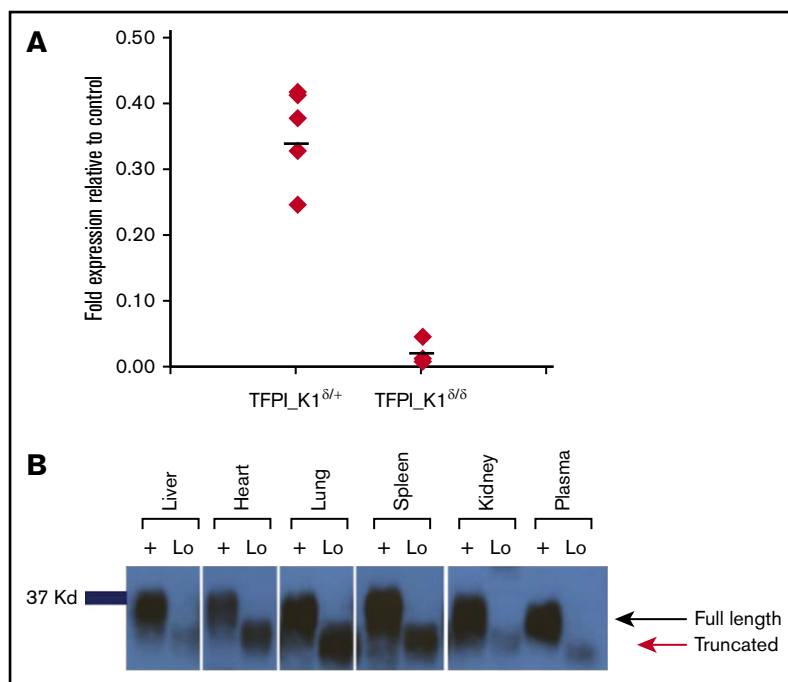
In the current work, we used the Meox2Cre strain¹⁸ to conditionally delete exon 4 of TFPI gene in epiblast-derived tissues while maintaining expression in trophoblast and primitive endoderm cells of the placenta (supplemental Figure 1). We have previously confirmed the excision pattern of Meox2Cre by using a double fluorescent Cre

reporter mouse.²² Meox2Cre^{tg/+} male mice were mated to TFPI_K1^{Lox/Lox} female mice to generate Meox2Cre^{tg/+} TFPI_K1 ^{δ /+} male mice. In a second cross, these were mated to TFPI_K1^{Lox/Lox} female mice. Equal frequencies of TFPI_K1^{Lox/+}, TFPI_K1^{Lox/ δ} , Meox2Cre^{tg/+} TFPI_K1 ^{δ /+} (abbreviated as TFPI_K1 ^{δ /+}), and Meox2Cre^{tg/+} TFPI_K1 ^{δ / δ} (abbreviated as TFPI_K1 ^{δ / δ}) genotypes are expected in progeny from this cross. The results indeed showed equal representation of these genotypes among embryos examined at 12.5 and 15.5 dpc and pups at weaning age (no significant difference was observed from expected Mendelian frequencies as determined by χ^2 GOF test, *P* = .514) (Table 1). TFPI_K1 ^{δ / δ} pups were born at 22% frequency with 95% CI of 16 to 28%. These results are in striking contrast to global TFPI K1 domain deletion, which results in complete embryonic lethality with no TFPI_K1^{-/-} pups surviving to wean.^{15,16} TFPI_K1 ^{δ / δ} embryos from epiblast-specific deletion were healthy in appearance with no obvious signs of bleeding or hemorrhage (Figure 1A-B).

Placentas of TFPI K1-deficient embryos do not show thrombotic or hemorrhagic abnormalities

We crossed TFPI_K1 ^{δ /+} male mice to WT C57BL/6 female mice to generate TFPI_K1^{+/-} animals. These animals contain a WT allele of TFPI and an exon 4-deleted allele in all cells. To replicate previously published observations with global deletion of TFPI K1 domain in mice, we examined 7 timed pregnancies from TFPI_K1^{+/-} intercrosses. We observed 6 TFPI_K1^{+/+}, 12 TFPI_K1^{+/-}, 2 TFPI_K1^{-/-}, and 7 aborted embryos (4 genotyped as TFPI_K1^{-/-}) at 11.5 and

Figure 3. RNA and protein expression in TFPI_K1^{δ/δ} mice. (A) Expression of exon 4 containing RNA in TFPI_K1^{δ/+} and TFPI_K1^{δ/δ} embryos relative to TFPI_K1^{Lox/+} litter mates is shown. TFPI_K1^{δ/δ} embryos show 95% to 99% reduction in exon 4 containing TFPI RNA. RNA was isolated from whole embryos. Primers specific for exon 4 were used for real-time qPCR analysis. (B) TFPI_K1^{δ/δ} mice express a truncated protein corresponding to K1-deleted TFPI. FXa-conjugated beads were used to pull down TFPI, and western immunoblotting was performed to evaluate the level of full-length protein in the organs of adult TFPI_K1^{δ/δ} mice (lanes marked "Lo") and WT C57Bl/6 controls (lanes marked "+"). No full-length TFPI protein could be detected in TFPI_K1^{δ/δ} mice. A truncated protein at reduced level of expression was readily detected.



8 TFPI_K1^{+/+}, 9 TFPI_K1^{+/-}, 3 TFPI_K1^{-/-}, and 3 aborted embryos (all genotyped as TFPI_K1^{-/-}) at 18.5 dpc. Thus, 58% of TFPI_K1^{-/-} embryos (7 out of 12) were found dead: 4 out of 6 at 11.5 and 3 out of 6 at 18.5. Of the 2 live embryos at 11.5, one showed intracranial hemorrhage, and both showed reduced elaboration of fetoplacental vasculature (Figure 2). Macroscopic placental hemorrhage was observed in another TFPI_K1^{-/-} embryo at 18.5 dpc (not shown). In contrast to these observations, the placentas corresponding to TFPI_K1^{δ/δ} embryos (generated using Meox2Cre) were grossly normal in appearance and in histology with no overt signs of excessive thrombotic lesions, bleeding, or abnormalities (Figure 1C-F). Thus, maintaining full-length TFPI expression in uteroplacental circulation corrected the placental abnormalities present in global TFPI K1 knockout mice.

Expression of truncated TFPI RNA and protein in TFPI K1 domain-deficient mice

To verify the efficiency of CRE recombinase-mediated excision of floxed exon 4, we performed real-time qPCR on reverse transcribed RNA extracted from whole embryos. The results demonstrated 95% to 99% reduction in exon 4 containing RNA in whole embryos (Figure 3A). We also conducted real-time qPCR on reverse transcribed RNA extracted from liver and kidneys of adult animals using primers encompassing exons 4 to 5. Results showed 95% to 99% reduction of exon 4 containing RNA. These results were visually confirmed by gel electrophoresis of the end products (supplemental Figure 2). A similar extent of TFPI exon 4 deletion was observed with real-time qPCR on genomic DNA from embryos and adult organs.

We used fXa-conjugated beads to pull down TFPI and performed western blot analysis to evaluate the level of full-length protein in adult TFPI_K1^{δ/δ} animals. No full-length TFPI protein was detected in the liver, heart, lung, spleen, kidney, or plasma of TFPI_K1^{δ/δ} mice. Instead, a truncated product corresponding to K1-deleted TFPI was

readily observed (Figure 3B). Thus, TFPI_K1^{δ/δ} mice lack detectable full-length TFPI protein expression.

TFPI K1-deficient mice show enhanced thrombin generation and are more susceptible to TF-induced pulmonary embolism

TFPI inhibits TF/FVIIa catalytic activity, and deletion of the Kunitz 1 domain results in loss of this inhibition. We measured the ability of TF and FVIIa to activate fX in vitro in the absence or presence of plasma from TFPI_K1^{δ/δ} or WT mice. This activity assay is sensitive to the presence of rTFPI. Factor X activation was significantly reduced in the presence of plasma from WT C57Bl/6 mice (64.2% ± 11.2% relative to no plasma control), whereas plasma from TFPI_K1^{δ/δ} mice had minimal effect (94.6% ± 5.1% relative to no plasma control) (supplemental Figure 3). We performed thrombin generation assay with platelet-poor plasma from TFPI_K1^{δ/δ} mice and WT controls. TFPI_K1^{δ/δ} mice showed reduced lag time as compared with WT controls (6 ± 0.98 minutes vs 7.9 ± 0.78 minutes; *P* < .006) and increased total thrombin generation as compared with controls in TF-initiated assays (2700 ± 616 nmol vs 216 ± 187 nmol, in WT controls; *P* < .0001) (Figure 4A). Notably, upon recalcification, platelet-poor plasma from TFPI_K1^{δ/δ} mice showed background thrombin generation in the absence of any added trigger (875 ± 696 nmol). Background thrombin generation was not observed in recalcified WT plasma without added trigger. These data are consistent with prothrombotic status of TFPI_K1^{δ/δ} mice. Measurement of TAT complexes revealed significantly higher TAT levels in TFPI_K1^{δ/δ} animals as compared with WT C57Bl/6 controls (3.8 ± 0.5 ng/mL vs 6.7 ± 1.9 ng/mL; *P* = .027) (Figure 4B).

We examined the effects of severe TFPI K1 deficiency on intravascular thrombosis by measuring their susceptibility to TF-induced pulmonary embolism compared with WT C57Bl/6 mice. Upon IV injection of TF, 4 out of 4 TFPI_K1^{δ/δ} mice exhibited respiratory arrest within 1 minute. In contrast, 6 of the 7 WT C57Bl/6

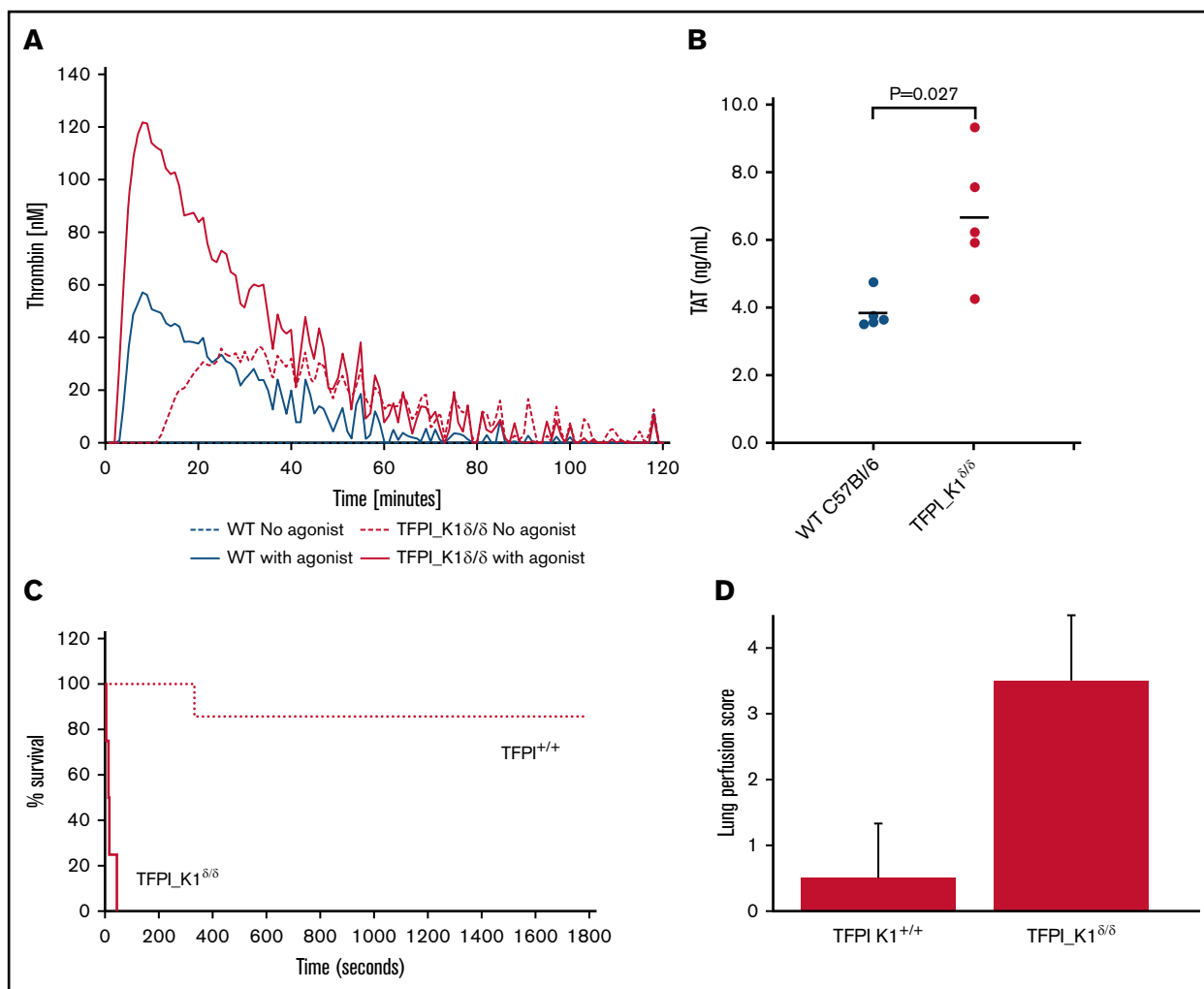


Figure 4. Evidence of prothrombotic tendency of TFPI_K1^{δ/δ} mice. (A) Plasma from TFPI_K1^{δ/δ} mice supports significantly enhanced thrombin generation as compared with plasma from WT C57Bl/6 mice. Thrombin generation assays conducted using TF as a trigger are shown for WT (blue solid line) and TFPI_K1-deficient plasma (red solid line). Background thrombin generation was observed in the absence of any added trigger in TFPI_K1-deficient (red dashed line), but not in WT plasma (blue dashed line). (B) Plasma TAT complex is elevated in TFPI_K1^{δ/δ} mice compared with WT controls. TAT levels in TFPI_K1-deficient and WT plasma were measured to be 3.8 ± 0.5 ng/mL vs 6.7 ± 1.9 ng/mL; mean ± standard deviation; P = .027. (C) Percent of surviving TFPI_K1^{δ/δ} mice (solid line) and WT (TFPI_K1^{+/+}) controls (dotted line) over time after IV injection of TF is shown. TFPI_K1^{δ/δ} mice are more susceptible to TF-induced pulmonary embolism as compared with controls (P = .006 at 30 minutes). (D) Lung perfusion scores (arbitrary units) with Evan's blue for TFPI_K1^{δ/δ} and control mice following TF injection are shown. TFPI_K1^{δ/δ} mice have significantly increased scores indicating increased perfusion defect (P = .003).

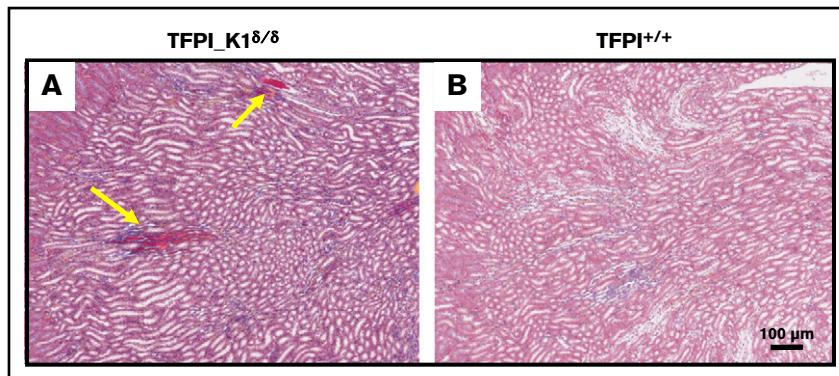
mice survived beyond 30 minutes; 1 WT C57BL/6 mouse died between 5 and 6 minutes following TF injection (Figure 4C). In addition to the end point of death, we assessed the degree of vascular occlusion of the lungs using Evan's blue perfusion assay. Lungs were scored for degree of perfusion as previously described.²¹ Lungs of most WT mice remained patent at the end of 30 minutes' observation (average score 0.5), whereas most TFPI_K1^{δ/δ} mice did not take up Evan's blue (average score 3.5) (Figure 4D; supplemental Figure 4).

Severe deficiency of TFPI K1 domain is associated with fibrin deposits in kidneys and rare instances of widespread brain ischemia

Carstairs' staining of histological sections of organs from TFPI_K1^{δ/δ} mice revealed fibrin deposits in kidneys of 5 out of 7 TFPI_K1^{δ/δ} mice

that were examined but not in 5 WT C57BL/6 controls (Figure 5). These results were confirmed with anti-(fibrin)ogen immunostaining (data not shown). Heart, liver, lungs, and spleen appeared unremarkable (data not shown). Of 43 TFPI_K1^{δ/δ} mice that were generated, 4 showed adverse events. Two were found dead during the sixth and ninth weeks, respectively. There was no evidence of overt thrombosis or hemorrhage in postmortem observation. Two others were found hunched, lethargic, trembling, and unable to move during the 14th and 16th weeks of age, respectively. These were euthanized, and organs were collected for qPCR and histological analysis. Interestingly, these mice had ≤1% residual full-length TFPI based on real-time qPCR on genomic DNA from liver and kidneys. Notably, these mice with extremely low TFPI did not have short or curly tails reported for complete absence of TFPI K1 domain.^{15,23} There were no obvious

Figure 5. Frequent fibrin deposits in renal medulla of TFPI_K1^{δ/δ} mice. Histological sections of kidneys from TFPI_K1^{δ/δ} (A) and WT C57Bl/6 control mice (B) with Carstairs' staining are shown. Bright orange/red stains in panel A (yellow arrows) are fibrin deposits seen in 5 out of 7 TFPI_K1^{δ/δ} mice examined, but in none of the 5 controls.



external signs of thrombosis in either mouse. Histological analysis of organs showed infarcted lesions in the brain in both mice, including in the cerebral cortex, brain stem, and hippocampus. Some lesions were old where neurons were replaced by gliotic scar tissue (Figure 6). Other lesions were estimated to be relatively recent, prior to gliosis and macrophage infiltration (supplemental Figure 5A-B), or showing infiltration of F4/80 positive macrophages (supplemental Figure 5C-F). These observations suggest that brain infarctions were a component of the acute illness observed in these animals. In addition, 1 mouse had an enlarged heart with an organized thrombus that stained positive for neutrophil/granulocyte marker Ly6G (supplemental Figure 6).

TFPI K1-deficient mice exhibit a normal life span and are fertile

Using Kaplan-Meier estimate and log-rank test, the TFPI_K1^{δ/δ} and control TFPI_K1^{δ/+} mice were found to have a comparable probability of adverse event-free survival analyzed up to 55 weeks ($P = .34$) (Figure 7). We tested whether TFPI_K1^{δ/δ} mice can carry pregnancies. TFPI_K1^{δ/δ} female mice were mated to WT C57Bl/6 male mice. This generated heterozygous progeny, allowing us to evaluate the effect of maternal TFPI deficiency alone. TFPI_K1^{δ/δ} female mice carried pregnancies successfully with litter sizes of 7.5 ± 1.6 (6 pregnancies of 2 female mice analyzed).

Discussion

In this study, we maintained TFPI expression in the uteroplacental circulation, but expression of full-length protein was disrupted in the fetoplacental circulation and in the embryo proper. The goal was to determine if this strategy would allow generation of mice that lack full-length TFPI and instead express a truncated protein missing the Kunitz-1 domain. We report that our strategy resulted in 95% to 99% deletion of exon 4 that encodes the Kunitz-1 domain. Mice with severe deficiency of full-length TFPI were viable and physically indistinguishable from their littermates. Most did not develop overt external signs of thrombotic or hemorrhagic episodes. Laboratory measurements revealed significantly elevated plasma TAT levels in TFPI_K1^{δ/δ} mice and increased thrombin generation potential measured in vitro. These mice were more susceptible to TF-induced pulmonary embolism than WT C57BL/6 controls. Histological evaluation and Carstairs' staining revealed frequent instances of fibrin deposition in their renal medulla. Two instances of severe brain ischemia associated with morbidity were observed among 43 TFPI_K1^{δ/δ} mice generated. These rare instances did not result in statistically significant difference in overall survival of

TFPI_K1^{δ/δ} mice compared with TFPI_K1^{δ/+} controls. Thus, TFPI_K1^{δ/δ} mice lived a normal life span. In addition, TFPI_K1^{δ/δ} female mice showed normal fertility and fecundity.

TF/FVIIa catalytic activity and Par4-mediated platelet activation are important determinants of embryonic lethality of TFPI K1 null mice.^{16,23,24} Platelets express TFPI α capable of binding early forms of FVa released by activated platelets and inhibiting the initial prothrombinase complex.^{9,25} Absence of this inhibition could result in local amplification of thrombin generation and platelet-mediated pathology. In the absence of Par4, TFPI K1 null mice show elevated TAT levels, but are protected from platelet activation and do not display overt thrombosis. Our results show that mice expressing 1% to 5% full-length TFPI also exhibit elevated TAT, but nonetheless survive in the presence of fully functional platelets and clotting system. These intriguing results suggest that TF/FVII inhibition provided by as little as 1% to 5% expression of TFPI is sufficient to put brakes on platelet-mediated coagulopathy associated with complete absence of TFPI K1.

The Cre-lox system has been widely used for making tissue-specific knockout mice; Meox2Cre provides an alternative to tetraploid aggregation by deleting LoxP-flanked DNA sequences in the

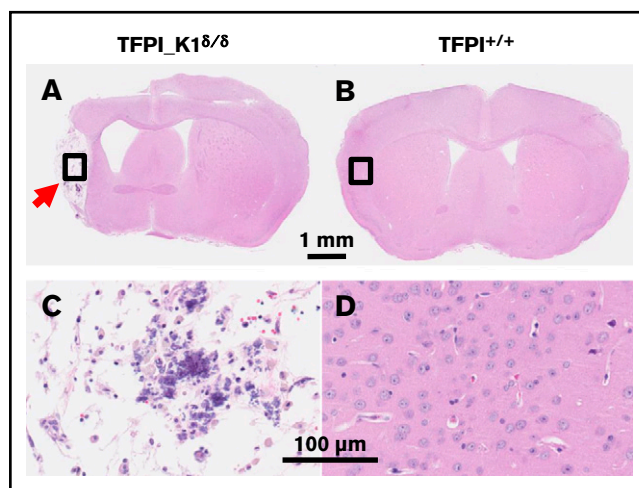


Figure 6. In rare instances, TFPI_K1^{δ/δ} mice exhibited large infarcted lesions in the brain. Hematoxylin and eosin-stained coronal sections and enlarged views of brains from a TFPI-deficient ($\leq 1\%$ residual full-length TFPI) (A,C) and WT control (B,D) mice are shown. Arrow points to an old lesion in the cerebral cortex replaced by scar tissue.

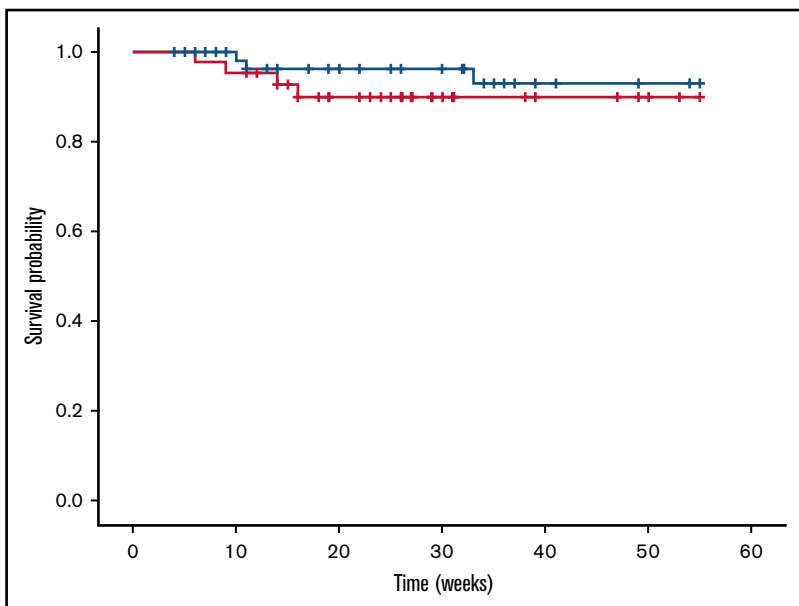


Figure 7. Kaplan-Meier disease-free survival curves for TFPI_K1^{Δ/Δ} and TFPI_K1^{Δ/+} mice. TFPI_K1-deficient mice (red line) exhibit a probability of adverse event-free survival comparable to heterozygous controls (black line) ($P = .37$). Censored observations (animals removed from the study) are indicated as cross lines. Two out of 43 TFPI_K1^{Δ/Δ} mice were found dead, and 2 others showed acute disease during the 14th and 16th weeks, but the probability of adverse event-free survival was not found to be significantly different from 73 controls of which 3 were found dead.

embryo with $\geq 95\%$ efficiency while maintaining them in the placenta. Although TFPI protein expression was below the limit of detection, residual 1% to 5% expression of full-length transcript was measured by qPCR. The Meox2Cre approach has been previously used by others and us to generate endothelial protein C receptor (PROCR)- and thrombomodulin (THBD)-deficient mice.^{22,26} In both cases, in utero survival of PROCR- and THBD-deficient mice made by Meox2Cre-Lox genetic approach contrasts with the embryonic loss of corresponding null mice generated by germline gene deletion. Low-level residual expression could, at least in part, be responsible for this contrast. Previous work by Castellino and colleagues has shown that very low expression of PROCR is sufficient for embryonic development and disease-free survival, in contrast to complete embryonic lethality in the absence of PROCR.²⁷ Taken together, it is likely that low-level residual expression of full-length TFPI contributes to embryonic and long-term survival of TFPI_K1^{Δ/Δ} mice.

About 60% TFPI K1 null mice die between 9.5 and 11.5 days of embryonic development, soon after the formation of the definitive placenta.¹⁵ Our results confirm this observation and also corroborate the previous finding that TFPI K1 null embryos show disrupted vascular network in the placenta.¹⁶ This defect is corrected in placentas of TFPI_K1^{Δ/Δ} mice, lending support to the notion that TFPI plays an essential role in the placenta. It, however, remains unclear if maintaining placental expression will be sufficient for survival of embryos with 100% TFPI gene disruption. Absence of FVII prolongs intrauterine survival of TFPI K1 null mice, whereas low TF or absence of Par4 results in live pups and adult mice.^{16,23,24} In each case, survival of TFPI K1 null mice is accompanied by concomitant reduction or absence of TF, FVII, or Par4 in the embryo. Careful reciprocal crosses and other genetic tools are needed to determine if preventing placental pathology alone will be sufficient to allow in utero development and postnatal survival of mice completely lacking TFPI K1 domain.

Inhibition of TFPI activity is being evaluated as a means to boost thrombin generation to compensate for the lack of FVIII or FIX in hemophilia patients.²⁸⁻³³ Our results suggest that inhibition of TFPI

K1 domain alone is sufficient to raise plasma TAT levels and increase the potential for fXa and thrombin generation. These observations lend support to the pursuit of K1-specific inhibition in prevention of bleeding in hemophilia patients.³¹ Though these therapies do not target complete inhibition, a potential risk is tipping the balance toward clotting. Our work has allowed an evaluation of possible developmental and hemostatic outcomes associated with inhibition of TFPI K1 domain activity in mice. Although severe TFPI K1 deficiency did not result in life-threatening thrombotic or hemorrhagic events, chronic fibrosis was indicated by the presence of frequent fibrin deposits in renal medulla. In addition, these mice could be susceptible to progressively increasing brain ischemia and infarction. Brain hemorrhage and diffuse fibrin deposition were previously reported in TFPI K1 null neonates, which survived embryonic development due to heterozygosity of FVII.²⁴ Interestingly, TFPI K1^{Δ/Δ} mice and embryos did not show short or curly tails observed in TFPI K1 knockout mice.^{15,23} We also note that in contrast to TFPI K1^{Δ/Δ} mice, two-thirds of THBD-deficient mice (generated using the same Meox2Cre strategy) succumbed to neonatal death, and the remaining succumbed to overt thrombosis.²² Thus, the absence of Thbd has a more severe impact on thrombotic propensity in C57BL/6 mice than the absence of TFPI K1 domain.

Our approach has allowed the generation of mice with severe deficiency of full-length TFPI without accompanying genetic alterations in coagulation- or inflammation-related molecules. Previous attempts to make TFPI K1 domain null mice had resulted in embryonic lethality.¹⁵ Adult null mice could be obtained if they were concomitantly deficient in TF or Par4, precluding evaluation of lack of TFPI K1 domain alone.^{16,23} Although overtly normal, mice severely deficient in TFPI K1 domain are prothrombotic. They provide a tool to study the role of TFPI K1 domain in physiological and disease processes, such as pregnancy, sepsis, and response to vascular injury.

Acknowledgments

The authors thank Michelle Bordas for maintaining the murine colony and for help with breeding experiments, Nicholas Martinez for

coordinating support from the Mast laboratory, the CRI Histology, Imaging and Pediatric Biobank and Analytical Tissue Core for expert services, and Andrew Webb and Ann Diamond for administrative support.

This work was supported by National Institutes of Health, National Heart, Lung, and Blood Institute grants HL112873 (R.S.) and HL068835 (A.E.M.).

Authorship

Contribution: M.M.C., Q.Y., M.Z., and R.S. designed and performed experiments and analyzed data; A.Y.P. helped with Kaplan-Meier survival analysis and log-rank test; M.W.L. examined and interpreted brain histology slides; A.E.M. provided critical reagents,

protocols, and suggestions; R.S. designed the study, interpreted data, and wrote the manuscript; and all authors reviewed the manuscript.

Conflict-of-interest disclosure: M.Z. is a current employee of MPP Group LLC. M.W.L. receives research support from and is a member of Scientific Advisory Boards for Audentes Therapeutics, Solid Biosciences, and Ichorion Therapeutics and is a consultant for Wave Life Sciences. A.E.M. receives research grant from Novo Nordisk. The remaining authors declare no competing financial interests.

Correspondence: Rashmi Sood, Medical College of Wisconsin, 8701 Watertown Plank Rd, Milwaukee, WI 53226; e-mail: rsood@mcw.edu.

References

1. Mast AE. Tissue factor pathway inhibitor: multiple anticoagulant activities for a single protein. *Arterioscler Thromb Vasc Biol.* 2016;36(1):9-14.
2. Edstrom CS, Calhoun DA, Christensen RD. Expression of tissue factor pathway inhibitor in human fetal and placental tissues. *Early Hum Dev.* 2000; 59(2):77-84.
3. Mast AE, Acharya N, Malecha MJ, Hall CL, Dietzen DJ. Characterization of the association of tissue factor pathway inhibitor with human placenta. *Arterioscler Thromb Vasc Biol.* 2002;22(12):2099-2104.
4. Sood R, Kalloway S, Mast AE, Hillard CJ, Weiler H. Fetomaternal cross talk in the placental vascular bed: control of coagulation by trophoblast cells. *Blood.* 2006;107(8):3173-3180.
5. Maroney SA, Ferrel JP, Pan S, et al. Temporal expression of alternatively spliced forms of tissue factor pathway inhibitor in mice. *J Thromb Haemost.* 2009;7(7):1106-1113.
6. Girard TJ, Warren LA, Novotny WF, et al. Functional significance of the Kunitz-type inhibitory domains of lipoprotein-associated coagulation inhibitor. *Nature.* 1989;338(6215):518-520.
7. Ndonwi M, Tuley EA, Broze GJ Jr. The Kunitz-3 domain of TFPI-alpha is required for protein S-dependent enhancement of factor Xa inhibition. *Blood.* 2010;116(8):1344-1351.
8. Hackeng TM, Seré KM, Tans G, Rosing J. Protein S stimulates inhibition of the tissue factor pathway by tissue factor pathway inhibitor. *Proc Natl Acad Sci USA.* 2006;103(9):3106-3111.
9. Wood JP, Bunce MW, Maroney SA, Tracy PB, Camire RM, Mast AE. Tissue factor pathway inhibitor-alpha inhibits prothrombinase during the initiation of blood coagulation. *Proc Natl Acad Sci USA.* 2013;110(44):17838-17843.
10. Wood JP, Petersen HH, Yu B, Wu X, Hilden I, Mast AE. TFPI α interacts with FVa and FXa to inhibit prothrombinase during the initiation of coagulation. *Blood Adv.* 2017;1(27):2692-2702.
11. Maroney SA, Ferrel JP, Collins ML, Mast AE. Tissue factor pathway inhibitor-gamma is an active alternatively spliced form of tissue factor pathway inhibitor present in mice but not in humans. *J Thromb Haemost.* 2008;6(8):1344-1351.
12. Duckers C, Simioni P, Spiezia L, et al. Low plasma levels of tissue factor pathway inhibitor in patients with congenital factor V deficiency. *Blood.* 2008; 112(9):3615-3623.
13. Sosa IR, Ellery P, Mast A, Neff AT, Gailani D. Acquired factor V deficiency in a patient without evidence of a classical inhibitor. *Haemophilia.* 2014;20(1): e81-e83.
14. Novotny WF, Brown SG, Miletich JP, Rader DJ, Broze GJ Jr. Plasma antigen levels of the lipoprotein-associated coagulation inhibitor in patient samples. *Blood.* 1991;78(2):387-393.
15. Huang ZF, Higuchi D, Lasky N, Broze GJ Jr. Tissue factor pathway inhibitor gene disruption produces intrauterine lethality in mice. *Blood.* 1997;90(3): 944-951.
16. Pedersen B, Holscher T, Sato Y, Pawlinski R, Mackman N. A balance between tissue factor and tissue factor pathway inhibitor is required for embryonic development and hemostasis in adult mice. *Blood.* 2005;105(7):2777-2782.
17. White TA, Johnson T, Zarzhevsky N, et al. Endothelial-derived tissue factor pathway inhibitor regulates arterial thrombosis but is not required for development or hemostasis. *Blood.* 2010;116(10):1787-1794.
18. Tallquist MD, Soriano P. Epiblast-restricted Cre expression in MORE mice: a tool to distinguish embryonic vs. extra-embryonic gene function. *Genesis.* 2000;26(2):113-115.
19. Sambrano GR, Weiss EJ, Zheng YW, Huang W, Coughlin SR. Role of thrombin signalling in platelets in haemostasis and thrombosis. *Nature.* 2001; 413(6851):74-78.
20. An J, Waitara MS, Bordas M, et al. Heparin rescues factor V Leiden-associated placental failure independent of anticoagulation in a murine high-risk pregnancy model. *Blood.* 2013;121(11):2127-2134.

21. Weiss EJ, Hamilton JR, Lease KE, Coughlin SR. Protection against thrombosis in mice lacking PAR3. *Blood*. 2002;100(9):3240-3244.
22. van Mens TE, Liang HH, Basu S, et al. Variable phenotypic penetrance of thrombosis in adult mice after tissue-selective and temporally controlled Thbd gene inactivation. *Blood Adv*. 2017;1(15):1148-1158.
23. Ellery PE, Maroney SA, Cooley BC, et al. A balance between TFPI and thrombin-mediated platelet activation is required for murine embryonic development. *Blood*. 2015;125(26):4078-4084.
24. Chan JC, Carmeliet P, Moons L, et al. Factor VII deficiency rescues the intrauterine lethality in mice associated with a tissue factor pathway inhibitor deficit. *J Clin Invest*. 1999;103(4):475-482.
25. Wood JP, Baumann Kreuziger LM, Ellery PER, Maroney SA, Mast AE. Reduced prothrombinase inhibition by tissue factor pathway inhibitor contributes to the factor V Leiden hypercoagulable state. *Blood Adv*. 2017;1(6):386-395.
26. Li W, Zheng X, Gu JM, et al. Extraembryonic expression of EPCR is essential for embryonic viability. *Blood*. 2005;106(8):2716-2722.
27. Castellino FJ, Liang Z, Volkir SP, et al. Mice with a severe deficiency of the endothelial protein C receptor gene develop, survive, and reproduce normally, and do not present with enhanced arterial thrombosis after challenge. *Thromb Haemost*. 2002;88(3):462-472.
28. Erhardtsen E, Ezban M, Madsen MT, et al. Blocking of tissue factor pathway inhibitor (TFPI) shortens the bleeding time in rabbits with antibody induced haemophilia A. *Blood Coagul Fibrinolysis*. 1995;6(5):388-394.
29. Gissel M, Orfeo T, Foley JH, Butenas S. Effect of BAX499 aptamer on tissue factor pathway inhibitor function and thrombin generation in models of hemophilia. *Thromb Res*. 2012;130(6):948-955.
30. Maroney SA, Cooley BC, Ferrel JP, et al. Absence of hematopoietic tissue factor pathway inhibitor mitigates bleeding in mice with hemophilia. *Proc Natl Acad Sci USA*. 2012;109(10):3927-3931.
31. Dockal M, Hartmann R, Fries M, et al. Small peptides blocking inhibition of factor Xa and tissue factor-factor VIIa by tissue factor pathway inhibitor (TFPI). *J Biol Chem*. 2014;289(3):1732-1741.
32. Willyard C. Thrombosis: Balancing act. *Nature*. 2014;515(7528):S168-S169.
33. Chowdary P, Lethagen S, Friedrich U, et al. Safety and pharmacokinetics of anti-TFPI antibody (concizumab) in healthy volunteers and patients with hemophilia: a randomized first human dose trial. *J Thromb Haemost*. 2015;13(5):743-754.